RSC Advances

PAPER

View Article Online
View Journal | View Issue

Check for updates

Cite this: *RSC Adv.*, 2017, **7**, 30640

Hydroquinone derivatives from the marine-derived fungus *Gliomastix* sp.†

Mohamed S. Elnaggar,[ab] Weaam Ebrahim,[ac] Attila Mándi,[d] Tibor Kurtán,[d] Werner E. G. Müller,[e] Rainer Kalscheuer,[a] Abdelnasser Singab,[b] Wenhan Lin,[f] Zhen Liu*[a] and Peter Proksch*[a]

Received 2nd May 2017
Accepted 3rd June 2017

DOI: 10.1039/c7ra04941b

rsc.li/rsc-advances

Eight new hydroquinone derivatives, gliomastins A–D (**1–4**), 9-*O*-methylgliomastin C (**5**), acremonin A 1-*O*-β-D-glucopyranoside (**6**), gliomastin E 1-*O*-β-D-glucopyranoside (**7**), and 6′-*O*-acetyl-isohomoarbutin (**8**), together with seven known analogues were isolated from the marine-derived fungus *Gliomastix* sp. Their structures were elucidated by extensive spectroscopic analysis including 1D and 2D NMR measurements aided by DFT NMR calculations as well as MS data. TDDFT-ECD and OR calculations were performed to determine the absolute configurations of **1** and the aglycones of **6** and **7**. Compound **1** features a novel skeleton, biogenetically derived from a Diels–Alder reaction between derivatives of **11** and **13**. Compound **2** represents a rare sulfur-containing alkaloid derived from the known hydroquinone **13**. Compounds **1**, **10** and **12** showed strong cytotoxicity against the L5178Y mouse lymphoma cell line with IC_{50} values of 1.8, 1.0 and 1.1 μM, respectively. Compound **3** exhibited moderate antitubercular activity against *Mycobacterium tuberculosis* with a MIC value of 12.5 μM.

Open Access Article. Published on 13 June 2017. Downloaded on 2/3/2025 8:55:51 PM.
This article is licensed under a Creative Commons Attribution 3.0 Unported Licence.

Introduction

Marine-derived microorganisms are attracting considerable attention owing to their high potential for producing new bioactive secondary metabolites.[1,2] Unique and stressful marine habitats, such as those characterized by extreme pressure, changing levels of salinity or temperature, may have a great impact on fungal biological activity.[3] One of the ecologically most diverse marine ecosystems are coral reefs.[4,5] In recent years, numerous bioactive secondary metabolites derived from coral-associated fungi have been reported.[3] Examples include the prenylated polyketides territrems A–C, which were isolated from the fungus *Aspergillus terreus* obtained from the gorgonian *Echinogorgia aurantiaca*, which exhibit pronounced acetylcholinesterase inhibitory activity.[6] Hydroanthraquinones and anthraquinone dimers, which were isolated from the soft coral-derived fungus *Alternaria* sp., showed cytotoxicity against PC-3 and HCT-116 tumor cell lines.[7] In addition, the structurally unique 14-membered resorcylic acid lactones cochliomycins A–C, which exhibit antifouling activity, were isolated from the gorgonian-derived fungus *Cochliobolus lunatus*.[8]

As a part of our ongoing exploration of bioactive metabolites from fungi,[9–12] examination of the Red Sea derived hard coral *Stylophora* sp. collected in Egypt, afforded different fungal strains from the coral tissues,[9] one of which was identified as *Gliomastix* sp. So far only few secondary metabolites have been reported from the genus *Gliomastix*, including the macrolides gliomasolide A–E,[13] the dihydroxanthenones muroxanthenone A–E,[14,15] as well as quinone/hydroquinone meroterpenoids.[16] The crude extract of the solid rice culture of *Gliomastix* sp. in this study showed cytotoxic activity against the L5178Y mouse lymphoma cell line with inhibition rate of 69.1% at a dose of 10 μg mL^{-1}. Chromatographic workup of the fungal extract afforded fifteen hydroquinone derivatives including eight new natural products (**1–8**). Herein, we report the isolation, structure elucidation as well as cytotoxic and antimicrobial activity of the isolated compounds.

Results and discussion

Compound **1** was isolated as a yellow amorphous powder. Its molecular formula was determined to be $C_{22}H_{22}O_4$ by HRESIMS, indicating twelve degrees of unsaturation. The ^{13}C NMR

[a]*Institute of Pharmaceutical Biology and Biotechnology, Heinrich-Heine-Universität Düsseldorf, 40225 Düsseldorf, Germany. E-mail: zhenfeizi0@sina.com; proksch@uni-duesseldorf.de*

[b]*Department of Pharmacognosy, Faculty of Pharmacy, Ain-Shams University, Cairo 11566, Egypt*

[c]*Department of Pharmacognosy, Faculty of Pharmacy, Mansoura University, Mansoura 35516, Egypt*

[d]*Department of Organic Chemistry, University of Debrecen, Debrecen 4032, Hungary*

[e]*Institute of Physiological Chemistry, Universitätsmedizin der Johannes Gutenberg-Universität Mainz, 55128 Mainz, Germany*

[f]*State Key Laboratory of Natural and Biomimetic Drugs, Peking University, Beijing 100191, P. R. China*

† Electronic supplementary information (ESI) available: UV, HRESIMS and NMR spectra of all the new compounds (**1–8**), NMR and ECD calculations for compound **1** as well as ECD and OR calculations for the aglycones of **6** and **7**. See DOI: 10.1039/c7ra04941b

This journal is © The Royal Society of Chemistry 2017

Open Access Article. Published on 13 June 2017. Downloaded on 2/3/2025 8:55:51 PM.
This article is licensed under a Creative Commons Attribution 3.0 Unported Licence.

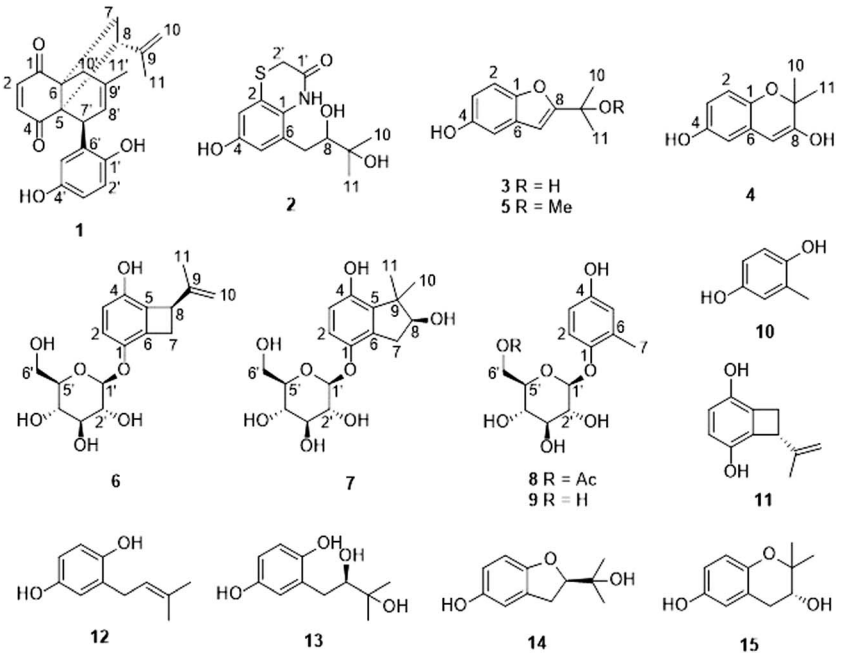

data of **1** (Table 1) together with HSQC and HMBC spectra revealed the presence of 22 carbons, including two carbonyl groups (δ_C 202.3 and 200.5), twelve olefinic or aromatic carbons (δ_C 110–151) and eight aliphatic carbons (two quaternary carbons at δ_C 59.8 and 47.6, two methines at δ_C 48.0 and 46.8, two methylenes at δ_C 36.9 and 36.5, and two methyls at δ_C 24.5 and 23.5). The ^{1}H NMR spectrum of **1** (Table 1) displayed five olefinic protons at 6.73 (d, H-2), 6.50 (d, H-3), 5.68 (br s, H-8′),

Table 1 NMR data for compounds **1** and **2**

	1[a]		**2**[a]	
Position	δ_C, type	δ_H (J in Hz)	δ_C, type[b]	δ_H (J in Hz)
1	202.3, C		129.8, C	
2	140.5, CH	6.73, d (10.4)	124.4, C	
3	142.2, CH[b]	6.50, d (10.4)	112.8, CH	6.65, d (2.6)
4	200.5, C		155.0, C	
5	59.8, C		117.0, CH	6.57, d (2.6)
6	47.6, C		132.6, C	
7	36.5, CH_2	2.66, dd (11.9, 10.6)	35.1, CH_2	2.80, dd (14.1, 1.6)
		1.97, dd (11.9, 8.8)		2.66, dd (14.1, 10.2)
8	48.0, CH	3.31[c]	81.6, CH	3.46, dd (10.2, 1.6)
9	145.8, C		73.4, C	
10	111.7, CH_2	4.83, s	25.9, CH_3	1.25, s
		4.66, s		
11	23.5, CH_3	1.77, s	24.1, CH_3	1.24, s
1′	148.3, C		167.6, C	
2′	117.1, CH	6.40, d (8.5)	30.8, CH_2	3.45, d (14.5)
				3.22, d (14.5)
3′	114.5, CH	6.34, dd (8.5, 2.9)		
4′	150.9, C			
5′	117.3, CH[b]	6.21, d (2.9)		
6′	130.8, C[b]			
7′	46.8, CH[b]	3.97, br s		
8′	122.7, CH[b]	5.68, br s		
9′	133.8, C			
10′	36.9, CH_2	2.97, d (17.7)		
		2.28, d (17.7)		
11′	24.5, CH_3	1.84, s		

[a] Recorded at 600 MHz for ^{1}H and 150 MHz for ^{13}C in CD_3OD. [b] Data extracted from HSQC and HMBC spectra. [c] Overlapped with water peak.

Open Access Article. Published on 13 June 2017. Downloaded on 2/3/2025 8:55:51 PM.
This article is licensed under a Creative Commons Attribution 3.0 Unported Licence.

4.83 (br s, H-10a) and 4.66 (br s, H-10b), representing a disubstituted double bond, a trisubstituted double bond and a terminal double bond, respectively. In addition, three aromatic protons of an ABX ring system at δ_H 6.40 (d, H-2′), 6.34 (dd, H-3′) and 6.21 (d, H-5′) as well as two methyls at 1.84 (s, Me-11′) and 1.77 (d, Me-11) were observed. These data accounted for nine degrees of unsaturation. Thus, compound **1** must possess a tricyclic skeleton in addition to an aromatic ring. The presence of a cyclohexenedione ring in **1** was established by the COSY correlation between H-2 and H-3 along with the HMBC correlations from H-2 to C-4 (δ_C 200.5) and C-6 (δ_C 47.6) and from H-3 to C-1 (δ_C 202.3) and C-5 (δ_C 59.8) (Fig. 1). The COSY correlations between H-7a (δ_H 2.66, dd)/H-8 (δ_H 3.31) and H-7b (δ_H 1.97, dd)/H-8 together with the HMBC correlations from H-7a to C-1, from H-7b to C-5, from H-8 to C-4 and C-5, and from Me-11 to C-8 (δ_C 48.0), C-9 (δ_C 145.8) and C-10 (δ_C 111.7) revealed that the cyclohexenedione ring was fused with a cyclobutane ring at the C-5 and C-6 positions and a isopropenyl group was attached at the C-8 position. In addition, the COSY correlation between H-7′ (δ_H 3.97)/H-8′ and the HMBC correlations from H-8′ to C-5, from Me-11′ to C-8′ (δ_C 122.7), C-9′ (δ_C 133.8) and C-10′ (δ_C 36.9), from H-10′a (δ_H 2.97, d) to C-1, and from H-10′b (δ_H 2.28, d) to C-5 and C-7 (δ_C 36.5) indicated a cyclohexene ring with a methyl substituent at the C-9′ position, which was fused with the cyclohexenedione ring through the C-5/C-6 bridge. Moreover, the presence of a benzene ring substituted at the C-7′ position was confirmed by the previous observation of an ABX aromatic spin system (H-2′, 3′ and 5′) and the HMBC correlations from H-2′ to C-4′ (δ_C 150.9) and C-6′ (δ_C 130.8), from H-3′ to C-1′ (δ_C 148.3) and C-5′ (δ_C 117.3), from H-5′ to C-3′ (δ_C 114.5), and from H-7′ to C-5′. Two hydroxy groups were suggested to be located at C-1′ and C-4′ as indicated by the chemical shifts of C-1′ and C-4′. Thus, the planar structure of **1** was elucidated as shown, for which the trivial name gliomastin A is proposed.

The relative configuration of **1** was determined by ROESY data (Fig. 1). The NOE correlations from H-7′ to H-8 and Me-11 suggested H-7′ and the cyclobutane ring to be on the same face of the cyclohexene ring while the NOE relationships between H-8/H-7b and H-7b/H-10′b indicated these protons to be orientated on the same side of the cyclobutane ring. In addition, DFT NMR calculations were performed on the arbitrarily chosen (5*S*,6*R*,8*R*,7′*R*)-**1** and (5*S*,6*R*,8*S*,7′*R*)-**1** epimers to decide between the (5*S**,6*R**,8*R**,7′*R**) and (5*S**,6*R**,8*S**,7′*R**) relative configuration of **1**. Merck Molecular Force Field (MMFF) conformational searches of the two epimers resulted in 14 and 14 low-energy conformers in a 21 kJ mol^{-1} energy window, respectively. These conformers were reoptimized at the B3LYP/6-31+G(d,p) level and NMR shift values were computed for conformers over 1% Boltzmann population at the mPW1PW91/6-311+G(d,p) level.[17] In accordance with the experimental NOE data, computed ^{13}C-NMR chemical shifts of most carbons suggest 8*S** relative configuration, while good agreement between experimental and computed ^{1}H-NMR chemical shifts of the 8*S** epimer compared to that of the 8*R** epimer allowed unambiguous assignment of the relative configuration of **1** as (5*S**,6*R**,8*S**,7′*R**).

To determine the absolute configuration of **1**, the solution TDDFT-ECD method was applied on the arbitrarily chosen (5*S*,6*R*,8*S*,7′*R*)-**1** enantiomer.[18,19] The 14 MMFF conformers obtained in the conformational search of the NMR calculations were reoptimized at the B3LYP/6-31G(d), B97D/TZVP[20,21] PCM/MeCN and CAM-B3LYP/TZVP[22,23] PCM/MeCN levels and ECD computations were performed for the low-energy conformers with various functionals (B3LYP, BH&HLYP, CAM-B3LYP, PBE0) combined with the TZVP basis set. Computed ECD spectra obtained at all of the applied combination of levels gave moderate to good mirror-image agreement with the experimental spectrum, allowing determination of the absolute configuration of **1** as (5*R*,6*S*,8*R*,7′*S*) (Fig. 2).

Gliomastin A (**1**) features a new carbon skeleton, which could be derived from two co-isolated known hydroquinone derivatives acremonin A (**11**)[24] and F-11334A$_1$ (**13**).[25,26] A biosynthetic pathway from the latter two compounds to **1** *via* Diels–Alder reaction is proposed (Fig. 3).

The molecular formula of compound **2** was established as $C_{13}H_{17}NO_4S$ by HRESIMS, requiring six degrees of unsaturation. In the ^{1}H NMR spectrum of **2** (Table 1), two *meta*-coupled aromatic protons at δ_H 6.65 (d, J = 2.6 Hz, H-3) and 6.57 (d, J = 2.6 Hz, H-5), one oxygenated methine at δ_H 3.46 (dd, J = 10.2, 1.6 Hz, H-8), one isolated methylene at δ_H 3.45 (d, J = 14.5 Hz,

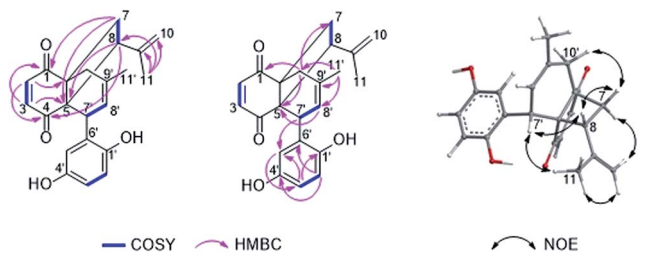

Fig. 1 Key COSY, HMBC and ROESY correlations of compound **1**.

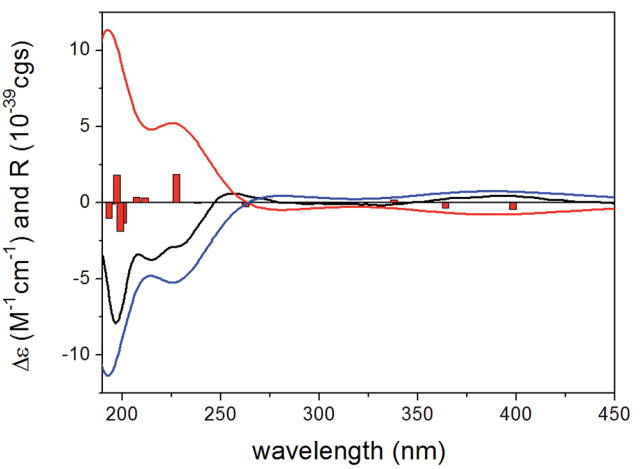

Fig. 2 Experimental ECD spectrum of **1** in MeCN (black line) compared with the B3LYP/TZVP ECD spectra computed for the B3LYP/6-31G(d) *in vacuo* optimized low-energy conformers of (5*S*,6*R*,8*S*,7′*R*)-**1** (average of 4 conformers, red line) and (5*R*,6*S*,8*R*,7′*S*)-**1** (average of 4 conformers, blue line). Bars represent computed rotational strength values of the lowest-energy conformer of (5*S*,6*R*,8*S*,7′*R*)-**1**.

This journal is © The Royal Society of Chemistry 2017

Open Access Article. Published on 13 June 2017. Downloaded on 2/3/2025 8:55:51 PM.
This article is licensed under a Creative Commons Attribution 3.0 Unported Licence.

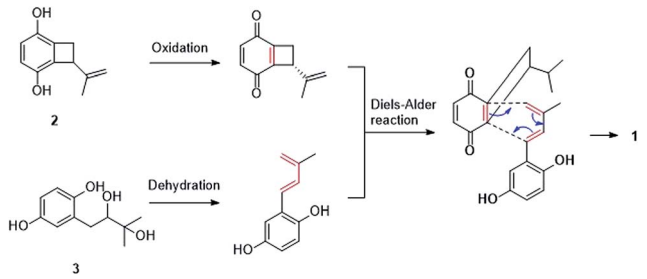

Fig. 3 A plausible biosynthetic pathway for compound **1**.

H-2′a) and 3.22 (d, $J = 14.5$ Hz, H-2′b), one methylene at δ_H 2.80 (dd, $J = 14.1$, 1.6 Hz, H-7a) and 2.66 (dd, $J = 14.1$, 10.2 Hz, H-7b), and two methyl groups at δ_H 1.25 (s, Me-10) and 1.24 (s, Me-11) were observed. The COSY correlations between H-7a/H-8 and H-7b/H-8 as well as the HMBC correlations from Me-10 and Me-11 to C-8 (δ_C 81.6) and C-9 (δ_C 73.4) indicated the presence of a 2,3-dihydroxy-3-methyl-butyl moiety in compound **2** (Fig. 4). The attachment of this moiety to a *meta*-coupled benzene ring at the C-6 position was confirmed by the HMBC correlations from H-7a and H-7b to C-1 (δ_C 129.8), C-5 (δ_C 117.0) and C-6 (δ_C 132.6), from H-3 to C-1, C-4 (δ_C 155.0) and C-5, and from H-5 to C-1, C-3 (δ_C 112.8), C-4 and C-7 (δ_C 35.1). C-4 was suggested to be substituted with a hydroxy group due to its high chemical shift. The HMBC correlations from H-2′a and H-2′b to C-2 (δ_C 124.4) and C-1′ (δ_C 167.6), combined with its molecular formula, indicated that the isolated methylene CH_2-2′ was linked to the benzene ring *via* an amide bond and a sulfur atom at the C-1 and C-2 positions to form an additional ring. Thus, the structure of **2** was determined, representing a rare sulfur-containing alkaloid, of which the co-isolated known hydroquinone derivative F-11334A$_1$ (**13**) could be the precursor.

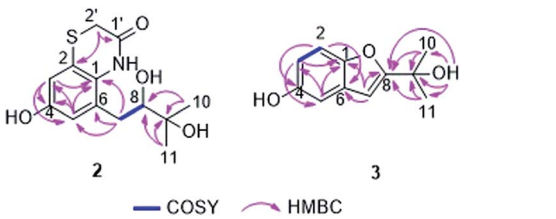

Fig. 4 Key COSY and HMBC correlations of compounds **2** and **3**.

Gliomastin C (**3**) was recovered as a white amorphous powder, possessing the molecular formula $C_{11}H_{12}O_3$ as determined by HRESIMS. Its ^{1}H NMR data (Table 2) exhibited three aromatic protons at δ_H 7.25 (d, $J = 8.8$ Hz, H-2), 6.95 (d, $J = 2.5$ Hz, H-5) and 6.76 (dd, $J = 8.8$, 2.5 Hz, H-3), which are characteristic signals of an ABX ring system. Together with the HMBC correlations from H-2 to C-4 (δ_C 154.1) and C-6 (δ_C 130.3), from H-3 to C-1 (δ_C 149.9) and C-5 (δ_C 106.4), and from H-5 to C-1 and C-3 (δ_C 113.0), a benzene ring in **3** was established (Fig. 4). Furthermore, the HMBC correlations from Me-10/11 to C-8 (δ_C 166.3) and C-9 (δ_C 69.1), from OH-9 (δ_H 4.32) to C-8, C-9 and C-10/11 (δ_C 29.4), and from H-7 (δ_H 6.52, s) to C-1, C-6 and C-8 indicated the nature of a 3-hydroxy-3-methyl-butenyl moiety and its attachment to C-6. A hydroxy group at C-4 and an oxygen bridge between C-1 and C-8 were assigned in consideration of the molecular formula and the chemical shifts of the corresponding carbons. Thus, the structure of gliomastin C (**3**) was elucidated as shown.

Gliomastin D (**4**) shared the same molecular formula as gliomastin C (**3**). The UV spectra and NMR data (Table 2) of **4** were also comparable to those of **3**. Three aromatic protons belonging to an ABX coupling system at δ_H 7.29 (d, H-2), 6.98 (d, H-5) and 6.80 (dd, H-3) were found in addition to a singlet olefinic methine at δ_H 6.63 (H-7) and two singlet methyls at δ_H 1.55 (Me-10 and 11). Analysis of the 1D and 2D NMR spectra of **4** revealed that the two compounds were structurally similar except for the position of the hydroxy group and the oxygen bridge. The upfield shifted C-8 (−4.4 ppm) and downfield shifted C-9 (+4.7 ppm) in **4** compared to those of **3** suggested the

Table 2 NMR data for compounds **3–5**

	3[a]		**4**[a]		**5**[b]	
Position	δ_C, type	δ_H (J in Hz)	δ_C, type	δ_H (J in Hz)	δ_C, type	δ_H (J in Hz)
1	149.9, C		150.1, C		150.8, C	
2	111.7, CH	7.25, d (8.8)	112.0, CH	7.29, d (8.8)	112.1, CH	7.25, d (8.8)
3	113.0, CH	6.76, dd (8.8, 2.5)	113.6, CH	6.80, dd (8.8, 2.5)	114.0, CH	6.74, dd (8.8, 2.5)
4	154.1, C		154.2, C		154.3, C	
5	106.4, CH	6.95, d (2.5)	106.4, CH	6.98, d (2.5)	106.7, CH	6.91, d (2.5)
6	130.3, C		129.9, C		130.2, C	
7	100.7, CH	6.52, s	104.4, CH	6.63, s	105.0, CH	6.61, s
8	166.3, C		161.9, C		161.5, C	
9	69.1, C		73.8, C		74.9, C	
10	29.4, CH_3	1.57, s	25.6, CH_3	1.55, s	25.6, CH_3	1.59, s
11	29.4, CH_3	1.57, s	25.6, CH_3	1.55, s	25.6, CH_3	1.59, s
OH-4		8.03, s		8.10, s		
OH-9		4.32, s				
OMe-9					51.3, CH_3	3.10, s

[a] Recorded at 600 MHz for ^{1}H and 150 MHz for ^{13}C in CD_3COCD_3. [b] Recorded at 600 MHz for ^{1}H and 150 MHz for ^{13}C in CD_3OD.

Open Access Article. Published on 13 June 2017. Downloaded on 2/3/2025 8:55:51 PM.
This article is licensed under a Creative Commons Attribution 3.0 Unported Licence.

presence of a pyran ring and a hydroxy group at C-8 in **4** instead of a furan ring.

Compound **5** was isolated as a white amorphous powder with the molecular formula $C_{12}H_{14}O_3$ as established by HRESIMS, containing an additional CH_2 unit compared to gliomastin C (**3**). The UV absorption spectrum and NMR data (Table 2) of **5** resembled those of **3** except for the appearance of an additional methoxy group at δ_C 51.3 and δ_H 3.10, which was further confirmed to be located at C-9 by the HMBC correlation from the protons of the methoxy group to C-8 (δ_C 74.9). Thus, compound **5** was elucidated as 9-*O*-methylgliomastin C.

The HRESIMS of compound **6** displayed a pseudomolecular ion peak at *m*/*z* 361.1255 $[M + Na]^+$, corresponding to the molecular formula $C_{17}H_{22}O_7$. Positive and negative ESIMS showed fragment peaks at *m*/*z* 177 $[M + H - 162]^+$ and 175 $[M - H - 162]^+$, respectively, which suggested the presence of a hexose residue in the molecule. The UV and NMR data (Table 3) of **6** were similar to those of acremonin A 4-*O*-β-D-glucopyranoside.[24] Acid hydrolysis of **6** yielded two products, one of which was confirmed to be the co-isolated hydroquinone acremonin A (**11**) by comparison of their NMR data and optical rotation values.[24] The other product was determined as β-D-glucopyranose by TLC analysis and optical rotation measurement compared to a known standard as well as by the *J* value (7.7 Hz) of the anomeric proton (H-1′) in **6**. Along with the 1D and 2D NMR spectra, compound **6** was unambiguously determined to contain an acremonin A moiety and a glucopyranose residue (Fig. 5). However, the HMBC correlations from H-1′ (δ_H 4.88, d) to C-1 (δ_C 146.6) rather than to C-4 (δ_C 147.2) indicated

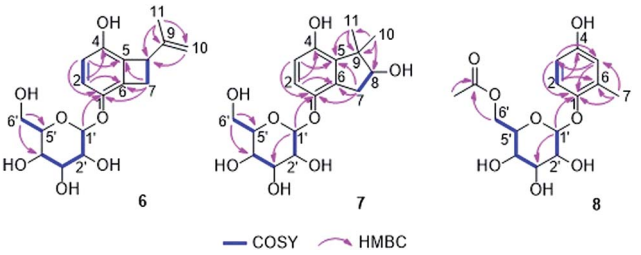

Fig. 5 Key COSY and HMBC correlations of compounds **6**, **7** and **8**.

that the glucopyranose residue was attached to C-1 instead of C-4. Thus compound **6** was elucidated as acremonin A 1-*O*-β-D-glucopyranoside.

Since the absolute configuration of acremonin A (**11**) is unknown in literature, ECD calculations were carried out for the arbitrarily chosen (*S*) enantiomer of the aglycone **11**. DFT reoptimization of the initial 15 MMFF conformers yielded 8 low-energy conformers at both the B3LYP/6-31G(d) *in vacuo* and the B97D/TZVP PCM/MeCN levels of theory. ECD spectra computed at various levels for these conformers gave nice mirror-image agreement with the experimental spectrum (Fig. 6). In some of the higher-energy conformers (*e.g.* conformers C and D, Fig. 7), the isopropenyl adopted a different orientation from that of the lowest-energy conformer, which is reflected in a near mirror image ECD of the conformers. Considering the relatively small computed energy differences of the conformers, this might be a possible source of error (energy difference between conformers A and C is less than 1 kJ mol^{-1}).[18,21] Therefore OR

Table 3 NMR data for compounds **6–8**

	6[a]		**7**[a]		**8**[a]	
Position	δ_C, type	δ_H (*J* in Hz)	δ_C, type[b]	δ_H (*J* in Hz)	δ_C, type[b]	δ_H (*J* in Hz)
1	146.6, C		148.6, C		150.4, C	
2	118.2, CH	6.69, d (8.8)	116.8, CH	6.80, d (8.7)	119.2, CH	6.92, d (8.7)
3	116.2, CH	6.54, d (8.8)	115.4, CH	6.50, d (8.7)	113.7, CH	6.52, dd (8.7, 3.0)
4	147.2, C		151.0, C		153.8, C	
5	132.8, C		136.9, C		118.1, CH	6.58, d (3.0)
6	129.8, C		131.4, C		131.0, C	
7	36.8, CH_2	3.55, dd (13.3, 5.7) 2.87, dd (13.3, 2.5)	36.3, CH_2	3.23, dd (16.1, 7.2) 2.70, dd (16.1, 7.2)	16.7, CH_3	2.21, s
8	48.9, CH	3.99, dd (5.7, 2.5)	82.2, CH	3.99, t (7.2)		
9	146.8, C		48.4, C			
10	110.6, CH_2	4.84, s 4.78, s	26.0, CH_3	1.36, s		
11	20.4, CH_3	1.78, s	20.0, CH_3	1.20, s		
1′	102.1, CH	4.88, d (7.7)	104.1, CH	4.69, d (7.6)	104.3, CH	4.66, d (7.6)
2′	75.0, CH	3.36, m	75.0, CH	3.41, m	75.1, CH	3.43, m
3′	77.9, CH	3.42, m	78.2, CH	3.42, m	78.0, CH	3.44, m
4′	71.4, CH	3.36, m	71.5, CH	3.35, m	71.7, CH	3.35, m
5′	78.2 CH	3.37, m	78.0 CH	3.32, m	75.2 CH	3.51, m
6′	62.6, CH_2	3.89, dd (12.2, 1.8) 3.69, dd (12.2, 5.2)	62.7, CH_2	3.87, dd (12.0, 2.1) 3.68, dd (12.0, 5.5)	64.7, CH_2	4.37, dd (11.8, 2.3) 4.25, dd (11.8, 6.6)
OAc-6′					172.7, C 20.7, CH_3	2.03, s

[a] Recorded at 600 MHz for ^1H and 150 MHz for ^{13}C in CD_3OD. [b] Data extracted from HSQC and HMBC spectra.

This journal is © The Royal Society of Chemistry 2017

Open Access Article. Published on 13 June 2017. Downloaded on 2/3/2025 8:55:51 PM.
This article is licensed under a Creative Commons Attribution 3.0 Unported Licence.

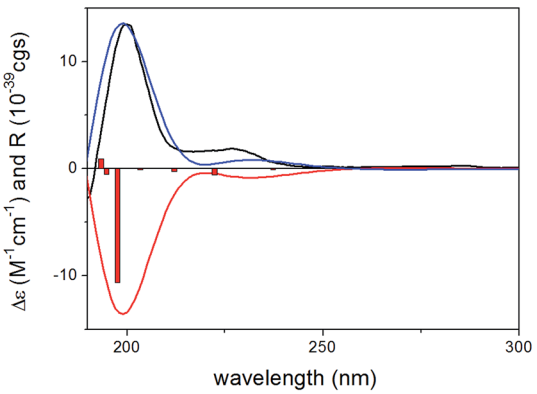

Fig. 6 Experimental ECD spectrum of **11** in MeCN (black line) compared with the PBE0/TZVP PCM/MeCN ECD spectra computed for the B97D/TZVP PCM/MeCN optimized low-energy conformers of (*S*)-**11** (average of 8 conformers/2, red line) and (*R*)-**11** (average of 8 conformers/2, blue line). Bars represent computed rotational strength values of (*S*)-**11** (conformer A/2).

calculations were also performed on the low-energy gas-phase conformers and on those reoptimized at the B97D/TZVP PCM/MeOH level (8 conformers over 2% also at this level).[27,28] The OR calculations performed at various levels for both sets of conformers were in line with the ECD results confirming the previous assignment. However, the sign of the OR values of the individual conformers were influenced by the orientation of isopropenyl group such as in the case of ECD. The (*R*) absolute configuration of the calculations was also confirmed by the biosynthetic relationship of **1** and **11**.

Compound **7** was obtained as a white solid. It possesses the molecular formula $C_{17}H_{24}O_8$ as established by analysis of the HRESIMS data. Similar to **6**, the NMR data (Table 3) of **7** exhibited two *ortho*-coupled aromatic protons at 6.80 (d, J = 8.7 Hz, H-2) and 6.50 (d, J = 8.7 Hz, H-3), signals of a methylene group at δ_H 3.23 (dd, J = 16.1, 7.2 Hz, H-7a) and 2.70 (dd, J = 16.1, 7.2 Hz, H-7b) and signals of a hexose residue including an anomeric proton at 4.69 (d, J = 7.6 Hz, H-1′). The nature of the benzene ring was established by the HMBC correlations from H-2 to C-4 (δ_C 151.0) and C-6 (δ_C 131.4) and from H-3 to C-1 (δ_C 148.6) and C-5 (δ_C 136.9) (Fig. 5). Analysis of the hydrolysis products of **7** confirmed the presence of a glucopyranose residue, which was determined to be attached to C-1 by the HMBC correlation from H-1′ to C-1. However, compared to **6**, the signals of the isopropenyl group were replaced by two singlet methyl groups at δ_H 1.35 (s, Me-10) and 1.20 (s, Me-11) as well as by an oxygenated methine at δ_C 82.2 and δ_H 3.99 (CH-8). The COSY correlations between H-7a/H-8 and H-7b/H-8 together with the HMBC correlations from Me-10 and Me-11 to C-5, C-8 and C-9 (δ_C 48.4), and from H-7a and H-7b to C-1, C-5 and C-6 indicated the presence of a further cyclopentene ring with two methyls at C-9 and a hydroxy group at C-8, which was fused to the benzene ring. Thus, the structure of **7** was elucidated as shown. Its aglycone was obtained following hydrolysis of **7**, representing a new hydroquinone derivative, for which the name gliomastin E is proposed.

For the configurational assignment of the aglycone gliomastin E, the solution TDDFT-ECD calculation protocol was carried out on the arbitrarily chosen (*S*) enantiomer. Reoptimization of the initial 23 MMFF conformers resulted in 13 and 15 low-energy (≥2%) conformers at the B3LYP/6-31G(d) *in vacuo* and the B97D/TZVP PCM/MeCN levels. ECD spectra computed at various levels for both sets of conformers resembled the 247 and the 198 nm transitions of gliomastin E suggesting (*S*) absolute configuration (Fig. 8). Since the 273 nm positive Cotton effect (CE) could not be reproduced by any of the applied combination, OR calculations performed *in vacuo* and in MeOH (similarly to **11**) were applied to prove the (*S*) absolute configuration.[28] OR values computed at all of the applied combinations of levels resulted in small positive overall optical rotations in the range from +10.2 to +18.4, while the experimental value was +15.2, which verified the ECD results.

The molecular formula $C_{15}H_{20}O_8$ was deduced for compound **8** from the HRESIMS data. The UV spectrum and

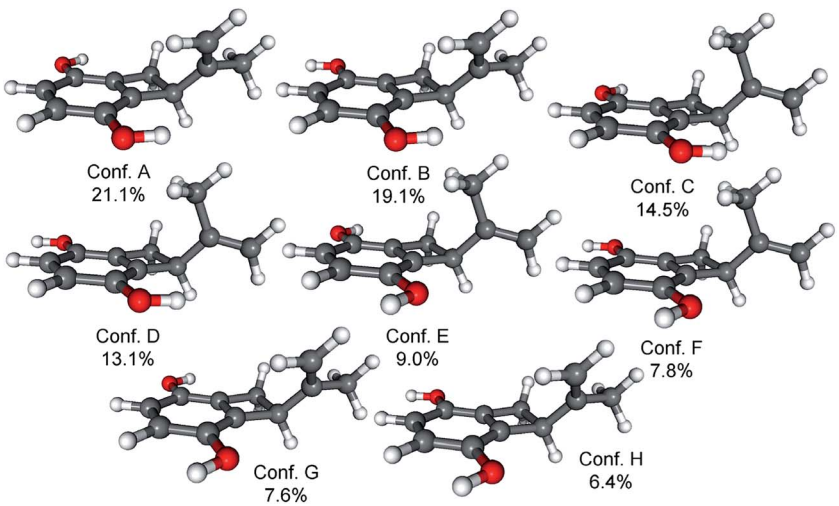

Fig. 7 Structures and populations of the low-energy (≥2%) B97D/TZVP PCM/MeCN conformers of (*S*)-**11**.

Open Access Article. Published on 13 June 2017. Downloaded on 2/3/2025 8:55:51 PM.
This article is licensed under a Creative Commons Attribution 3.0 Unported Licence.

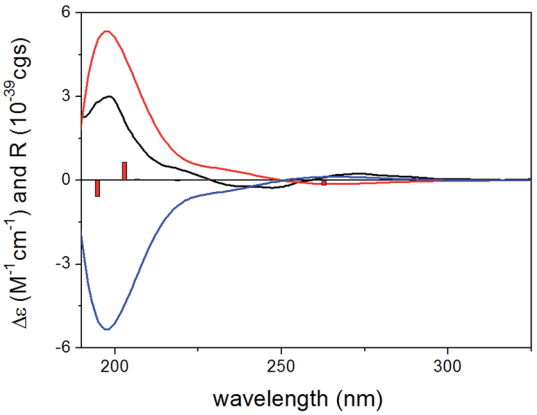

Fig. 8 Experimental ECD spectrum of gliomastin E in MeCN (black line) compared with the B3LYP/TZVP ECD spectra computed for the B3LYP/6-31G(d) *in vacuo* optimized low-energy conformers of (*S*)-gliomastin E (average of 13 conformers, red line) and (*R*)-gliomastin E (average of 13 conformers, blue line). Bars represent computed rotational strength values of the lowest-energy conformer of (*S*)-gliomastin E.

NMR data (Table 3) of **8** were almost identical to those of isohomoarbutin (**9**),[29,30] except for the appearance of an additional acetoxy group (δ_H 2.03, δ_C 20.7 and 172.7) in **8**. This acetoxy group was determined to be located at C-6′ on the basis of the HMBC correlations from H-6′a and H-6′b (δ_H 4.37 and 4.25) to the carbonyl carbon of the acetoxy group. The remaining structure of **8** was confirmed to be the same as **9** by detailed analysis of the 2D NMR spectra of **8** (Fig. 5). The hexose residue was determined to be β-D-glucopyranose by the coupling constant (7.6 Hz) of the anomeric proton (H-1′) and analysis of the acid hydrolysis products of **8** in comparison with a known standard. Owing to the data mentioned above, compound **8** was elucidated as 6′-*O*-acetyl-isohomoarbutin.

By comparison with the literature data, the remaining known compounds were identified as isohomoarbutin (**9**),[29,30] 2-methyl-1,4-benzenediol (**10**),[31] acremonin A (**11**),[24] prenylhydroquinone (**12**),[32,33] F-11334A$_1$ (**13**),[25,26] (*R*)-2-(2-hydroxypropan-2-yl)-2,3-dihydro-5-hydroxybenzofuran (**14**),[34] and 2,2-dimethylchroman-3,6-diol (**15**).[24]

All isolated compounds (**1–15**) were evaluated for their cytotoxicity against the L5178Y murine lymphoma cell line (Table 4). Compounds **1**, **10**, **12** and **13** showed significant cytotoxic activity with IC_{50} values of 1.8, 1.0, 1.1 and 3.0 μM, respectively, which are below that of the positive control kahalalide F. Compared to the two precursors **11** and **13**, compound **1** demonstrated stronger cytotoxicity while the sulfur-containing alkaloid **2** was inactive compared to its precursor **13**. Compounds **10** and **11** showed strong cytotoxicity while their glycosides **8**, **9** and **6** were inactive. The ether bridge in **14** and **15** led to total loss of cytotoxicity compared to **13**.

In addition, all compounds were tested for their antitubercular activity against *Mycobacterium tuberculosis* and for their antibacterial activities against different strains of pathogenic bacteria (Table 4). Only compounds **10** and **12** exhibited antibacterial activity but they were also cytotoxic. Compound **3**, which lacked cytotoxicity, showed antitubercular activity with a MIC value of 12.5 μM. Comparison of the antitubercular activity of **3** with those of **4**, **5**, **14** and **15** indicated the importance of the furan ring and of the free hydroxy group at C-9.

In conclusion, our investigation of secondary metabolites from the marine-derived fungus *Gliomastix* sp. led to the isolation of fifteen hydroquinone derivatives including eight new natural products (**1–8**). Among the latter, the dimer **1** possesses a novel carbon skeleton, which could be derived from derivatives of **11** and **13** through a Diels–Alder reaction. Compound **1** also exhibited significant cytotoxicity against the L5178Y mouse lymphoma cell line with an IC_{50} value of 1.8 μM. Compound **2** is a rare sulfur-containing alkaloid. TDDFT-ECD and OR calculations were performed to determine the absolute configurations of **1** and the aglycones of **6** and **7**. All isolated compounds were tested for their cytotoxic and antimicrobial activity and the structure–activity relationships were discussed.

Experimental section

General procedures

Optical rotations were recorded on a PerkinElmer-241 MC polarimeter. ^{1}H, ^{13}C and 2D NMR spectra were measured on a Bruker Avance DMX 600 NMR spectrometer. A Finnigan LCQ

Table 4 Cytotoxicity, antitubercular and antibacterial activities of **1**, **3**, **10–13**

	Cytotoxicity IC_{50} (μM)	Antitubercular and antibacterial MIC (μM)						
Compd	L5178Y	TB	*S. aureus* ATCC 25923	*S. aureus* ATCC 700699	*E. faecalis* ATCC 29212	*E. faecalis* ATCC 51299	*E. faecium* ATCC 35667	*E. faecium* ATCC 700221
1	1.8	—	—	—	—	—	—	—
3	—[a]	12.5	—	—	—	—	—	—
10	1.0	12.5	25	6.25	12.5	12.5	12.5	25
11	9.6	25	—	—	—	—	—	—
12	1.1	12.5	25	12.5	12.5	6.25	6.25	12.5
13	3.0	25	—	—	—	—	—	—
Positive control	4.3[b]	<0.64[c]	1.56[d]	1.56[d]	0.008[e]	0.008[e]	0.008[e]	0.008[e]

[a] IC_{50} or MIC > 50 μM. [b] Kahalalide F as positive control. [c] Rifampicin as positive control. [d] Moxifloxacin as positive control. [e] Ciprofloxacin as positive control.

This journal is © The Royal Society of Chemistry 2017

Open Access Article. Published on 13 June 2017. Downloaded on 2/3/2025 8:55:51 PM.
This article is licensed under a Creative Commons Attribution 3.0 Unported Licence.

Deca XP Thermoquest spectrometer was used to record mass spectra while a FTHRMS-Orbitrap (Thermo Finnigan) mass spectrometer was utilized to obtain HRESIMS data. The Dionex P580 HPLC system was coupled to a photodiode array detector (UVD340S) and the analytical column (125 × 4 mm, L x i.d.) was prefilled with Eurospher-10 C_{18} (Knauer, Germany). Semi-preparative HPLC separation was performed on a Lachrom-Merck Hitachi HPLC system (Pump L7100, UV detector L7400 and Eurosphere 100 C_{18} column: 300 × 8 mm) with 5.0 mL min^{-1} flow rate. Normal phase column chromatography was carried out using Merck MN Silica gel 60 M (0.04–0.063 mm) or Sephadex LH-20. TLC was carried out on precoated Silica Gel 60 F254 plates (Merck, Germany) with UV detection at 254 and 365 nm as well as following spraying with anisaldehyde reagent or with methanol–sulfuric acid (95 : 5).

Fungal material and identification

The hard coral *Stylophora* sp. was obtained from the Red Sea in Egypt near the coastline of Ain El-Sokhna area in November 2012. The fungal strain was isolated from the freshly crushed inner tissues of the coral following standard procedures and was identified as *Gliomastix* sp. according to a molecular biological protocol that was carried out through DNA amplification and sequencing of ITS region as described previously.[9,35] The obtained data of sequencing were submitted to GenBank with the accession number KX354951. A voucher strain was deposited in the Institute of Pharmaceutical Biology and Biotechnology, Heinrich-Heine University, Düsseldorf, Germany, with the ID code ST-F3.

Cultivation, extraction and isolation

Fungal biomass fermentation was performed in Erlenmeyer flasks (15 × 1 L, each contains 100 g rice of commercially available rice and 110 mL water, which was kept overnight before being autoclaved for 20 min at a temperature of 121 °C) on solid rice medium at 25 °C under static conditions for 30 d. Harvesting process started with soaking the culture of each flask in EtOAc (500 mL), in addition to cutting the culture mass into small pieces using a spatula. The flasks were then kept overnight and subjected to shaking at 150 rpm for 8 h on the next day. The obtained extract was subjected to filtration, and evaporated to obtain a dark brown crude extract (6.5 g).

This crude extract was partitioned between *n*-hexane and 90% aqueous methanol and the resulting methanolic phase was evaporated to give 4.5 g of methanolic extract, which was further chromatographed over silica gel using vacuum liquid chromatography (VLC). Gradient elution with *n*-hexane–EtOAc (100 : 0 to 0 : 100) and CH_2Cl_2–MeOH (100 : 0 to 0 : 100) was used and 500 mL eluting volume for each fraction was collected to obtain fifteen subfractions (F1–F15).

F4 (750 mg) was subjected to a Sephadex LH-20 (100 × 5 cm) column using MeOH as eluent to obtain six subfractions (F4-1–F4-6), of which F4-5 (80 mg) was purified using semi-preparative RP-HPLC with 60% MeOH–H_2O as mobile phase to yield compounds **10** (42.3 mg), **11** (3.6 mg) and **12** (13.0 mg).

F5 (120 mg) was further fractionated using a Sephadex LH-20 column (80 × 4 cm) with MeOH as eluent to give five subfractions (F5-1–F5-5). Subfraction F5-1 (34 mg) was subjected to semi-preparative RP-HPLC with 38% MeOH–H_2O to yield **15** (14.0 mg) and **14** (3.2 mg). Subfraction F5-2 (14 mg) was purified by semi-preparative RP-HPLC using 50% MeOH–H_2O to give **5** (1.5 mg). Subfraction F5-3 (10 mg) was separated by semi-preparative RP-HPLC using 57% MeOH–H_2O to afford **3** (0.9 mg) and **4** (2.4 mg). Subfraction F5-4 (15 mg) was purified by semi-preparative RP-HPLC with 64% MeOH–H_2O as mobile phase to yield **1** (3.5 mg).

Following similar procedures, compound **13** (7.4 mg) was obtained from fraction F8, by column chromatography over a Sephadex LH-20 column (100 × 5 cm) with MeOH as eluent, followed by purification using semipreparative RP-HPLC with 34% MeOH–H_2O.

F10 (235 mg) was separated into five subfractions (F10-1–F10-5) by a Sephadex LH-20 column (80 × 4 cm) using 100% MeOH as eluent. Subfraction F10-3 (35 mg) was then subjected to semi-preparative RP-HPLC eluted with 40% MeOH–H_2O to yield **9** (1.8 mg) and **8** (3.0 mg) while subfraction F10-4 (13 mg) was purified by semi-preparative RP-HPLC with 50% MeOH–H_2O to afford **2** (0.8 mg).

Compounds **7** (2.2 mg) and **6** (3.0 mg) were obtained from fraction F12 (150 mg) using a Sephadex LH-20 column (80 × 4 cm) with MeOH for elution followed by semi-preparative HPLC separation with 35% MeOH–H_2O as eluent.

Gliomastin A (1). Yellow amorphous powder; $[\alpha]_D^{20}$ −6 (*c* 0.37, MeOH); UV (MeOH) λ_{max}: 212 and 296 nm; ECD {MeCN, λ_{max} ($\Delta\varepsilon$) *c* 0.35 mM} 392 (+0.46), 372sh (+0.34), 331 (−0.18), 272sh (+0.27), 255 (+0.60), 228sh (−2.88), 215sh (−3.75), 197 (−7.91) nm; ^{1}H NMR and ^{13}C NMR data, see Table 1; HRESIMS $[M + Na]^+$ *m*/*z* 373.1412 (calcd for $C_{22}H_{22}O_4Na$, 373.1410).

Gliomastin B (2). White solid;$[\alpha]_D^{20}$ +24 (*c* 0.08, MeOH); UV (MeOH) λ_{max}: 211, 243 and 292 nm; ^{1}H NMR and ^{13}C NMR data, see Table 1; HRESIMS $[M + H]^+$ *m*/*z* 284.0950 (calcd for $C_{13}H_{18}NO_4S$, 284.0951).

Gliomastin C (3). White amorphous powder; UV (MeOH) λ_{max}: 203, 249 and 294 nm; ^{1}H NMR and ^{13}C NMR data, see Table 2; HRESIMS $[M + Na]^+$ *m*/*z* 215.0677 (calcd for $C_{11}H_{12}O_3Na$, 215.0679).

Gliomastin D (4). White amorphous powder; UV (MeOH) λ_{max}: 206, 249 and 295 nm; ^{1}H NMR and ^{13}C NMR data, see Table 2; HRESIMS $[M - H_2O + H]^+$ *m*/*z* 175.0751 (calcd for $C_{11}H_{11}O_2$, 175.0754).

9-*O*-Methylgliomastin C (5). White amorphous powder; UV (MeOH) λ_{max}: 206, 249 and 295 nm; ^{1}H NMR and ^{13}C NMR data, see Table 2; HRESIMS $[M - H]^-$ *m*/*z* 205.0870 (calcd for $C_{12}H_{13}O_3$, 205.0870).

Acremonin A 1-*O*-β-D-glucopyranoside (6). White amorphous powder;$[\alpha]_D^{20}$ +30 (*c* 0.31, MeOH); UV (MeOH) λ_{max}: 206 and 298 nm; ^{1}H NMR and ^{13}C NMR data, see Table 3; HRESIMS $[M + Na]^+$ *m*/*z* 361.1255 (calcd for $C_{17}H_{22}O_7Na$, 361.1258).

Gliomastin E 1-*O*-β-D-glucopyranoside (7). White solid;$[\alpha]_D^{20}$ +22 (*c* 0.33, MeOH); UV (MeOH) λ_{max}: 201 and 281 nm; ^{1}H NMR and ^{13}C NMR data, see Table 3; HRESIMS $[M + Na]^+$ *m*/*z* 379.1361 (calcd for $C_{17}H_{24}O_8Na$, 379.1363).

Open Access Article. Published on 13 June 2017. Downloaded on 2/3/2025 8:55:51 PM.
This article is licensed under a Creative Commons Attribution 3.0 Unported Licence.

6′-*O*-Acetyl-isohomoarbutin (8). White amorphous powder; $[\alpha]_D^{20}$ +10 (*c* 0.31, MeOH); UV (MeOH) λ_{max}: 201, 214 and 283 nm; ^{1}H NMR and ^{13}C NMR data, see Table 3; HRESIMS $[M + Na]^+$ *m*/*z* 351.1053 (calcd for $C_{15}H_{20}O_8Na$, 351.1050).

Acremonin A (11). $[\alpha]_D^{20}$ +138 (*c* 0.37, MeOH); ECD {MeCN, λ_{max} ($\Delta\varepsilon$) *c* 0.71 mM} 286sh (+0.30), 227sh (+1.90), 200 (+13.49) nm.

Gliomastin E (aglycone of 7). $[\alpha]_D^{20}$ +15 (*c* 0.05, MeOH); ECD {MeCN, λ_{max} ($\Delta\varepsilon$) *c* 0.70 mM} 273 (+0.24), 247 (−0.26), 198 (+3.01) nm.

Acid hydrolysis

Compounds **6–8** (1 mg each) were separately hydrolyzed with 2 N HCl (2.0 mL) at 90 °C for 4 h. After cooling, the solution was partitioned with EtOAc (3 mL × 3) and H_2O. The EtOAc phase containing the aglycone was dried under reduced pressure. The water phase containing the sugar moiety, was then examined using TLC analysis with D-glucose as an authentic standard (Sigma-Aldrich, Germany). Two different eluting systems were used including DCM–MeOH–H_2O (6 : 4 : 1) and EtOAc–MeOH–H_2O (10 : 4 : 1), along with methanol–sulphuric acid as spraying reagent.

Cytotoxicity assay

The MTT method was performed to test the cytotoxicity of the compounds against the L5178Y mouse lymphoma cell line (European Collection of Authenticated Cell Cultures, Catalogue No. 87111908) as described previously.[36] Kahalalide F was used as positive control and media with 0.1% DMSO was used as negative control.

Antibacterial assay

The antibacterial assay was performed using the broth microdilution method. Following the recommendations of the Clinical and Laboratory Standards Institute (CLSI), the MIC values against *S. aureus* ATCC 25923, *S. aureus* ATCC 700699, *E. faecalis ATCC 29212, E. faecalis* ATCC 51299, *E. faecium* ATCC 35667, *E. faecium* ATCC 700221 and *Mycobacterium tuberculosis* strain H37Rv were determined.[37] Moxifloxacin (for *S. aureus* strains), ciprofloxacin (for *E. faecalis and E. faecium* strains) and rifampicin (for *Mycobacterium tuberculosis*) were used as positive controls.

Computational section

Mixed torsional/low-frequency mode conformational searches were carried out by means of the Macromodel 9.9.223 software using the Merck Molecular Force Field (MMFF) with an implicit solvent model for $CHCl_3$.[38] Geometry reoptimizations were carried out at the B3LYP/6-31G(d) level *in vacuo*, the B3LYP/6-31+G(d,p) level *in vacuo*, the B97D/TZVP[20,21] and the CAMB3LYP/TZVP[22,23] levels with the PCM solvent model for MeCN or MeOH. TDDFT ECD calculations and OR calculations were run with various functionals (B3LYP, BH&HLYP, CAM-B3LYP, PBE0) and the TZVP basis set as implemented in the Gaussian 09 package with the same or no solvent model as in the preceding DFT optimization step.[39] NMR calculations were performed at the mPW1PW91/6-311+G(2d,p) level.[17] ECD spectra were generated as sums of Gaussians with 3000 and 3300 cm^{-1} widths at half-height (corresponding to *ca.* 12 and 13 nm at 200 nm), using dipole-velocity-computed rotational strength values.[40] Computed ECD spectra were shifted by −48 (B3LYP/TZVP for the B3LYP/6-31G(d) *in vacuo* conformers) for **1**, +6 (PBE0/TZVP PCM/MeCN for the B97D/TZVP PCM/MeCN conformers) for **11** and −3 (B3LYP/TZVP for the B3LYP/6-31G(d) *in vacuo* conformers) for gliomastin E. Computed C-NMR data were corrected with $I = 185.4855$ and $S = -1.0306$ and H-NMR data with $I = 31.8996$ and $S = -1.0734$.[41,42] Boltzmann distributions were estimated from the ZPVE-corrected B3LYP/6-31G(d) energies in the B3LYP/6-31G(d) gas-phase calculations, and from the uncorrected B3LYP/6-31+G(d,p), B97D/TZVP and CAM-B3LYP/TZVP energies in the other cases. The MOLEKEL software package was used for visualization of the results.[43]

Acknowledgements

A scholarship granted and financed by the Egyptian government (Ministry of High Education) to M. S. E. is gratefully acknowledged. Financial support by the DFG (GRK 2158) to P. P. and R. K. is gratefully acknowledged. T. K. and A. M. thank the National Research, Development and Innovation Office (NKFI K120181 and PD121020) for financial support and the Governmental Information-Technology Development Agency (KIFÜ) for CPU time.

Notes and references

1 J. W. Blunt, B. R. Copp, R. A. Keyzers, M. H. G. Munro and M. R. Prinsep, *Nat. Prod. Rep.*, 2014, **31**, 160–258.
2 M. E. Rateb and R. Ebel, *Nat. Prod. Rep.*, 2011, **28**, 290–344.
3 X. M. Hou, R. F. Xu, Y. C. Gu, C. Y. Wang and C. L. Shao, *Curr. Med. Chem.*, 2015, **22**, 3707–3762.
4 T. A. Richards, M. D. M. Jones, G. Leonard and D. Bass, *Annual Review of Marine Science*, 2012, **4**, 495–522.
5 W. Chen, Y. Li and Y. Guo, *Acta Pharm. Sin. B*, 2012, **2**, 227–237.
6 F. He, J. Bao, X. Y. Zhang, Z. C. Tu, Y. M. Shi and S. H. Qi, *J. Nat. Prod.*, 2013, **76**, 1182–1186.
7 C. J. Zheng, C. L. Shao, Z. Y. Guo, J. F. Chen, D. S. Deng, K. L. Yang, Y. Y. Chen, X. M. Fu, Z. G. She, Y. C. Lin and C. Y. Wang, *J. Nat. Prod.*, 2012, **75**, 189–197.
8 C. L. Shao, H. X. Wu, C. Y. Wang, Q. A. Liu, Y. Xu, M. Y. Wei, P. Y. Qian, Y. C. Gu, C. J. Zheng, Z. G. She and Y. C. Lin, *J. Nat. Prod.*, 2011, **74**, 629–633.
9 M. S. Elnaggar, S. S. Ebada, M. L. Ashour, W. Ebrahim, W. E. G. Müller, A. Mándi, T. Kurtán, A. Singab, W. Lin, Z. Liu and P. Proksch, *Tetrahedron*, 2016, **72**, 2411–2419.
10 M. S. Elnaggar, S. S. Ebada, M. L. Ashour, W. Ebrahim, A. Singab, W. Lin, Z. Liu and P. Proksch, *Fitoterapia*, 2017, **116**, 126–130.
11 W. Ebrahim, M. El-Neketi, L. I. Lewald, R. S. Orfali, W. Lin, N. Rehberg, R. Kalscheuer, G. Daletos and P. Proksch, *J. Nat. Prod.*, 2016, **79**, 914–922.

 This journal is © The Royal Society of Chemistry 2017

Open Access Article. Published on 13 June 2017. Downloaded on 2/3/2025 8:55:51 PM.
This article is licensed under a Creative Commons Attribution 3.0 Unported Licence.

12 S. Liu, H. Dai, G. Makhloufi, C. Heering, C. Janiak, R. Hartmann, A. Mándi, T. Kurtán, W. E. G. Müller, M. U. Kassack, W. Lin, Z. Liu and P. Proksch, *J. Nat. Prod.*, 2016, **79**, 2332–2340.
13 J. Zhang, X. P. Lin, L. C. Li, B. L. Zhong, X. J. Liao, Y. H. Liu and S. H. Xu, *RSC Adv.*, 2015, **5**, 54645–54648.
14 H. Y. Yang, D. Y. Niu, L. Wang, S. J. Wang, C. M. Zhang, X. M. Gao, G. Du and Q. F. Hu, *J. Asian Nat. Prod. Res.*, 2015, **17**, 319–323.
15 W. Dong, C. Liu, Q. Shen, T. Zhang, Y. Wang, K. Zhou, B. Ji, H. Yang, G. Du, Q. Hu and M. Zhou, *Chem. Nat. Compd.*, 2016, **52**, 620–623.
16 W. J. He, X. J. Zhou, X. C. Qin, Y. X. Mai, X. P. Lin, S. R. Liao, B. Yang, T. Zhang, Z. C. Tu, J. F. Wang and Y. Liu, *Nat. Prod. Res.*, 2017, **31**, 604–609.
17 C. Adamo and V. Barone, *J. Chem. Phys.*, 1998, **108**, 664–675.
18 G. Pescitelli and T. Bruhn, *Chirality*, 2016, **28**, 466–474.
19 A. Mándi, I. W. Mudianta, T. Kurtán and M. J. Garson, *J. Nat. Prod.*, 2015, **78**, 2051–2056.
20 S. Grimme, *J. Comput. Chem.*, 2006, **27**, 1787–1799.
21 P. Sun, D. X. Xu, A. Mándi, T. Kurtán, T. J. Li, B. Schulz and W. Zhang, *J. Org. Chem.*, 2013, **78**, 7030–7047.
22 T. Yanai, D. Tew and N. Handy, *Chem. Phys. Lett.*, 2004, **393**, 51–57.
23 G. Pescitelli, L. Di Bari and N. Berova, *Chem. Soc. Rev.*, 2011, **40**, 4603–4625.
24 A. Abdel-Lateff, G. M. König, K. M. Fisch, U. Höller, P. G. Jones and A. D. Wright, *J. Nat. Prod.*, 2002, **65**, 1605–1611.
25 M. Tanaka, F. Nara, Y. Yamasato, Y. Ono and T. Ogita, *J. Antibiot.*, 1999, **52**, 827–830.
26 L. Shen, S. D. Zhao and H. J. Zhu, *Gaodeng Xuexiao Huaxue Xuebao*, 2011, **32**, 2568–2573.
27 P. L. Polavarapu, *Chirality*, 2008, **20**, 664–672.
28 P. Sun, Q. Yu, J. Li, R. Riccio, G. Lauro, G. Bifulco, T. Kurtán, A. Mándi, H. Tang, C. L. Zhuang, W. H. Gerwick and W. Zhang, *J. Nat. Prod.*, 2016, **79**, 2552–2558.
29 H. Thieme, *Pharmazie*, 1970, **25**, 129.
30 E. Walewska and H. Thieme, *Pharmazie*, 1969, **24**, 423.
31 H. M. Chawla, S. K. Sharma, K. Chakrabarty and S. Bhanumati, *Tetrahedron*, 1988, **44**, 1227–1234.
32 Y. C. Chien, C. H. Lin, M. Y. Chiang, H. S. Chang, C. H. Liao, I. S. Chen, C. F. Peng and I. L. Tsai, *Phytochemistry*, 2012, **80**, 50–57.
33 S. Yamada, F. Ono, T. Katagiri and J. Tanaka, *Bull. Chem. Soc. Jpn.*, 1977, **50**, 750.
34 W. J. Lan, W. Liu, W. L. Liang, Z. Xu, X. Le, J. Xu, C. K. Lam, D. P. Yang, H. J. Li and L. Y. Wang, *Mar. Drugs*, 2014, **12**, 4188–4199.
35 J. Kjer, A. Debbab, A. H. Aly and P. Proksch, *Nat. Protoc.*, 2010, **5**, 479–490.
36 M. Ashour, R. Edrada, R. Ebel, V. Wray, W. Wätjen, K. Padmakumar, W. E. G. Müller, W. H. Lin and P. Proksch, *J. Nat. Prod.*, 2006, **69**, 1547–1553.
37 CLSI, *Methods for Dilution Antimicrobial Susceptibility Tests for Bacteria That Grow Aerobically; Approved Standard–Ninth Edition*, Clinical and Laboratory Standards Institute, 2012.
38 MacroModel; Schrödinger, LLC, 2012, http://www.schrodinger.com/MacroModel.
39 M. J. Frisch, G. W. Trucks, H. B. Schlegel, G. E. Scuseria, M. A. Robb, J. R. Cheeseman, G. Scalmani, V. Barone, B. Mennucci, G. A. Petersson, H. Nakatsuji, M. Caricato, X. Li, H. P. Hratchian, A. F. Izmaylov, J. Bloino, G. Zheng, J. L. Sonnenberg, M. Hada, M. Ehara, K. Toyota, R. Fukuda, J. Hasegawa, M. Ishida, T. Nakajima, Y. Honda, O. Kitao, H. Nakai, T. Vreven, J. A. Montgomery Jr, J. E. Peralta, F. Ogliaro, M. Bearpark, J. J. Heyd, E. Brothers, K. N. Kudin, V. N. Staroverov, R. Kobayashi, J. Normand, K. Raghavachari, A. Rendell, J. C. Burant, S. S. Iyengar, J. Tomasi, M. Cossi, N. Rega, J. M. Millam, M. Klene, J. E. Knox, J. B. Cross, V. Bakken, C. Adamo, J. Jaramillo, R. Gomperts, R. E. Stratmann, O. Yazyev, A. J. Austin, R. Cammi, C. Pomelli, J. W. Ochterski, R. L. Martin, K. Morokuma, V. G. Zakrzewski, G. A. Voth, P. Salvador, J. J. Dannenberg, S. Dapprich, A. D. Daniels, Ö. Farkas, J. B. Foresman, J. V. Ortiz, J. Cioslowski and D. J. Fox, *Gaussian 09, Revision B.01*, Gaussian, Inc., Wallingford, CT, 2010.
40 P. J. Stephens and N. Harada, *Chirality*, 2010, **22**, 229–233.
41 CHESHIRE CCAT, the Chemical Shift Repository for computed NMR scaling factors, http://cheshirenmr.info/index.htm.
42 M. W. Lodewyk, M. R. Siebert and D. J. Tantillo, *Chem. Rev.*, 2012, **112**, 1839–1862.
43 U. Varetto, *MOLEKEL, v. 5.4*, Swiss National Supercomputing Centre, Manno, Switzerland, 2009.